

Noise Characterization of an Injection-Locked Titanium:sapphire  
Laser System

Daniel Adam Thrasher

A senior thesis submitted to the faculty of  
Brigham Young University  
in partial fulfillment of the requirements for the degree of  
Bachelor of Science

Scott D. Bergeson, Advisor

Department of Physics and Astronomy

Brigham Young University

July 2013

Copyright © 2013 Daniel Adam Thrasher

All Rights Reserved

## ABSTRACT

### Noise Characterization of an Injection-Locked Titanium:sapphire Laser System

Daniel Adam Thrasher  
Department of Physics and Astronomy  
Bachelor of Science

This thesis reports amplitude and frequency noise measurements of a Titanium:sapphire (Ti:sapphire) laser that is injection-locked with a low power diode laser. We use a heterodyne technique to frequency off-set lock a home built injection-locked Ti:sapphire laser with a low noise, commercial, injection-locked Ti:sapphire laser. Frequency noise measurements are made using the full-width-half-max of the two lasers' beat note. Amplitude noise measurements are made using the root mean square (rms) of the output of a photo diode. Under optimal conditions the rms amplitude noise is 1.0% and the frequency noise is 300 kHz . The noise of our laser system depends on the feedback system characteristics. My contributions were the design and fabrication of a microwave interferometer, including its software and hardware, for the purpose of frequency off-set locking the two lasers. I also contributed to the data acquisition and analysis.

Keywords: injection locking, titanium:sapphire, phase noise, amplitude noise

## ACKNOWLEDGMENTS

Special thanks to Dr. Scott Bergeson for his inspiration and tutelage as well as Matt Burbidge for his assistance.

This research is funded in part by the National Science Foundation, grant number PHY-0969856

# Contents

|  |           |
|--|-----------|
| <b>Table of Contents</b>                               | <b>iv</b> |
| <b>List of Figures</b>                                 | <b>v</b>  |
| <b>1 Introduction</b>                                  | <b>1</b>  |
| 1.1 Overview . . . . .                                 | 1         |
| 1.2 Injection Locking . . . . .                        | 2         |
| 1.3 Frequency and Amplitude Noise . . . . .            | 2         |
| 1.4 Heterodyne Technique . . . . .                     | 3         |
| <b>2 Experimental Setup</b>                            | <b>6</b>  |
| 2.1 Laser Setup . . . . .                              | 6         |
| 2.2 Microwave Interferometer . . . . .                 | 8         |
| <b>3 Results</b>                                       | <b>14</b> |
| 3.1 Frequency Noise Measurements . . . . .             | 14        |
| 3.2 Amplitude Noise Measurements . . . . .             | 17        |
| 3.3 Discussion: Regenerative Amplifier Model . . . . . | 19        |
| 3.4 Conclusion . . . . .                               | 20        |
| <b>Bibliography</b>                                    | <b>22</b> |
| <b>Index</b>   | <b>23</b> |

# List of Figures

|     |   |    |
|-----|---|----|
| 2.1 | Experimental setup for frequency noise measurements. . . . .  | 7  |
| 2.2 | Layout for diagnostic interferometer . . . . .  | 9  |
| 2.3 | VCO frequency as a function of resistance . . . . .   | 10 |
| 2.4 | VCO frequency excursion before temperature controlling . . . . .  | 11 |
| 2.5 | VCO frequency excursion after temperature control modifications . . . . .                               | 12 |
| 2.6 | Beat note frequency as a function of the interferometer's phase shift . . . . .                         | 13 |
| 3.1 | Beat note frequency noise between diode seed and commercial Ti:sapphire lasers .                        | 15 |
| 3.2 | Beat note frequency noise between the injection-locked seed and commercial Ti:sapphire lasers . . . . . | 16 |
| 3.3 | Amplitude noise of injection-locked laser with 80 mW seed power . . . . .                               | 17 |
| 3.4 | Amplitude noise of injection-locked laser with 15 mW seed power . . . . .                               | 18 |

# Chapter 1

## Introduction

### 1.1 Overview

In 2002, an injection-locked Ti:sapphire laser, wherein a low power diode laser was amplified by a large bandwidth amplifier laser, was demonstrated [1, 2]. The system is of interest to the laser physics community because of its broad amplification bandwidth. In 2006, further diagnostics were performed on a similar injection-locked system by another research group [3]. This analysis concluded that the poor phase noise inherent in diode lasers is converted to amplitude noise as a result of the injection locking process and is not sufficiently suppressed by conventional feedback systems. This analysis further concluded that the laser system was consequently not suitable for quantum optic experimentation. As such a conclusion might discourage the wide implementation of this amplifier, this thesis presents both frequency and amplitude noise measurements of the amplifier as well as a discussion on a conventional feedback system which successfully suppressed the amplitude noise.

I presented this research at the 2010 APS Four Corners Meeting in Ogden, UT, the 2011 Spring Research Conference at BYU, as well as the 2011 meeting of the APS Division of Atomic Molec-

ular and Optical Physics in Atlanta, GA. Our findings were subsequently published in the Journal of Applied Optics B.

## 1.2 Injection Locking

Injection locking can be used to amplify a low-power diode laser to Watt-level power with excellent spatial mode quality (e.g., the majority of the output light is in the TEM<sub>00</sub> Gaussian mode). The injection-locked laser system consists of a seed laser, generally low power and of the desired frequency; and an amplifying laser, generally a laser with broad bandwidth, piezoelectric crystal adjustment, and significantly higher power. For a power-amplifier laser cavity to amplify light of a specific wavelength, the cavity must meet a resonance condition: the round-trip optical path length within the cavity must be equal to an integer of the seed laser's specific wavelength. This resonance condition is maintained using the Pound-Drever-Hall technique [4], wherein an error signal produced by the phase change in the seed laser relative to the power-amplifier cavity is integrated to produce an electronic correction to the seed laser frequency, thus maintaining resonance according to the power amplifier cavity length.

## 1.3 Frequency and Amplitude Noise

Noise is undesired or uncontrolled change in a system. We measure both frequency and amplitude noise. Amplitude noise is the excursion of the laser's amplitude or intensity over some time scale. We measure laser amplitude noise using a fast photodetector (Thor labs DET36A). We discuss the amplitude noise in terms of the root-mean-square of the Fourier transform of the amplitude excursions over a particular time interval. Similarly, frequency noise is the excursion of the laser's frequency over some time interval. Unlike amplitude noise, we measure frequency noise relative to another more stable (less noisy) laser using a heterodyne technique, explained in section 1.4. If

we model our laser as emitting only a very narrow frequency spectrum at a given time, then the frequency noise is how much this narrow spectrum changes over some time interval relative to our stable laser. We discuss frequency noise in terms of the full-width-half-maximum (FWHM) of the heterodyne signal.

## 1.4 Heterodyne Technique

Heterodyning is the process of combining signals in order to acquire information about them. We can deduce the frequency excursions of our home-built injection-locked Ti:sapphire laser using a heterodyne technique. This is accomplished by mixing the oscillating electric fields of a commercial injection-locked laser and our home-built laser to create a beat note or difference frequency. We use the oscillating electric field of a commercial injection-locked laser because of its low frequency noise.

If we model our two lasers as oscillating electric fields using Euler's method we have,

$$Laser_1 = \frac{e^{i\omega_1 t} + e^{-i\omega_1 t}}{2} \quad Laser_2 = \frac{e^{i\omega_2 t} + e^{-i\omega_2 t}}{2}.$$

Where  $\omega_1$  and  $\omega_2$  are the respective laser frequencies and  $t$  is time. A photo diode acts like a mixer when two lasers are overlapped onto it. Its AC output  $P$  is the relative product of the two laser fields,

$$P = \left[ \frac{e^{i\omega_1 t} + e^{-i\omega_1 t}}{2} \right] \left[ \frac{e^{i\omega_2 t} + e^{-i\omega_2 t}}{2} \right],$$

which yields

$$P = \cos [t(\omega_1 + \omega_2)] + \cos [t(\omega_1 - \omega_2)].$$

The first term contains the sum of the two frequencies. Since these are optical frequencies, their sum (approx. 10 PHz) is much too fast to be measured by the photodetector. Hence we can ignore it. The second term above is the beat note or difference frequency. If the frequency

of this difference frequency does not change in time, then we say that the frequency of our two lasers is locked. We can stabilize this beat note so its center frequency does not change in time using a frequency offset lock [5]. Our frequency lock is a microwave interferometer. It allows us to eliminate long-term drift in the beat note through electronic feedback. The output of the interferometer is an error signal which maintains the beat note frequency by writing changes onto the amplifier laser cavity length.

The interferometer accomplishes this by splitting the beat note signal and sending the signals through two different lengths of co-axial cable,  $L_1$  and  $L_2$ . The two different lengths of co-axial cable induce a relative phase change between the two signals. If we model our beat note  $B_1(t)$  using Euler's method we have,

$$B_1(t) = \frac{e^{i(\omega t + \phi)} + e^{-i(\omega t + \phi)}}{2}.$$

Where  $\omega$  is the beat frequency and  $\phi$  is its phase. The signal from the mixer is the product of two phase shifted signals

$$B_2(t) = \left[ \frac{e^{i(\omega t + 2\pi n L_1 / \lambda)} + e^{-i(\omega t + 2\pi n L_1 / \lambda)}}{2} \right] \left[ \frac{e^{i(\omega t + 2\pi n L_2 / \lambda)} + e^{-i(\omega t + 2\pi n L_2 / \lambda)}}{2} \right],$$

which yields,

$$B_2(t) = \frac{1}{2} \cos \left[ 2\omega t + \frac{2\pi n}{\lambda} (L_1 + L_2) \right] + \frac{1}{2} \cos \left[ \frac{2\pi n}{\lambda} (L_1 - L_2) \right].$$

Where  $L_1$  and  $L_2$  are the two cable lengths,  $n$  is the index of refraction of the cable, and  $\lambda$  is the beat wavelength. The first term is eliminated using a low-pass filter, changing the interferometer's output to

$$\tilde{B}_2(t) = \frac{1}{2} \cos \left[ \frac{2\pi n}{\lambda} (L_1 - L_2) \right].$$

This is the interferometer error signal. It is a DC signal which is dependent on the input beat note frequency (or wavelength) as well as the relative cable lengths ( $L_1 - L_2$ ). It is a measure of how

well the center frequency of our beat note is stabilized. Changes due to noise in our home-built injection-locked laser's frequency are converted to phase changes in the error signal. We utilize this signal in a negative feedback circuit which changes the length of the piezoelectric crystal within the amplifying laser cavity in order to make the difference signal as small as possible.

# Chapter 2

## Experimental Setup

### 2.1 Laser Setup

Here we discuss the experimental set-up and operation, which allowed us to make the aforementioned measurements. We also discuss the data acquisition process for acquiring frequency and amplitude noise data.

The home-built Ti:sapphire cavity is the exact same cavity from [1] (the original demonstration experiment). Because the focus of this thesis is the noise characterization of the laser system, as well as the fact that I did not build the laser cavity, I do not list the cavity components explicitly here. They can be found in [1].

For amplitude noise measurements, the light from our home-built injection-locked Ti:sapphire laser is measured using a DC-1 GHz bandwidth detector which is then read using a digital oscilloscope set to acquire 1 Mega points at a rate of 1 Giga sample/second. These data are acquired from the oscilloscope using a labVIEW program. Noise floor measurements were taken following every measurement by blocking the laser and measuring the un-illuminated detector. This noise floor was then subtracted from the laser's data. We found that engaging the frequency off-set lock

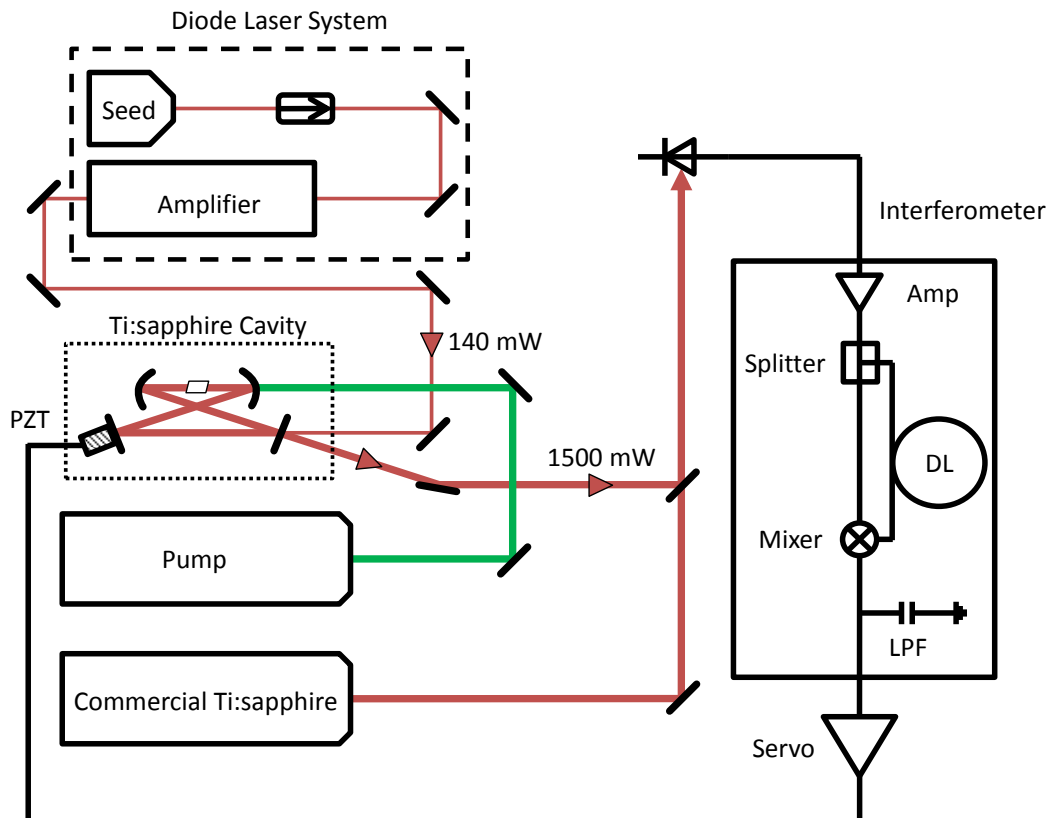


**Figure 2.1** Experimental setup for frequency noise measurements. The feedback loop from the Pound Drever Hall (PDH) lock is not shown. Although the light in our free running Ti:sapphire cavity naturally propagates in both directions, we force it to propagate as shown by locking the diode laser to it. Acronyms are as follows: Amp- Amplifier, LPF- Low Pass Filter, DL- Delay Line

had no noticeable influence on the amplitude noise measurements.

For frequency noise measurements, a portion of the output beam from our home-built injection-locked Ti:sapphire laser is overlapped (i.e. made co-linear) with a portion of the output beam from a commercial Ti:sapphire laser (manufactured by  $M^2$  with a center frequency at 846 nm and 1.5 W output power) onto a photodiode. It is important that these two laser beams are co-linear, in order for their electric fields to properly interfere one with another. The signal from this detector, or beat note, is first recorded by our oscilloscope and then enters the aforementioned interferometer. The output of the interferometer, or error signal, is sent to a servo (amplifier) which feeds back to the piezoelectric crystal within our home-built Ti:sapphire cavity, thus frequency locking our home-built laser with the commercial laser.

The FWHM of the beat note measured by our oscilloscope is the frequency noise of our home-built laser relative to the commercial laser. During preliminary data acquisition we found that our beat note measurements had unexpected noise levels. We concluded via trail and error that these were a result from noise in the error signal. We cleaned up the error signal by installing a 10.1 MHz bandpass filter before the interferometer. This addition dramatically improved the error signal's accuracy.

## **2.2 Microwave Interferometer**

To mitigate long term wavelength drift in the injection-locked Ti:sapphire laser, it was expedient that the phase shift induced by our microwave interferometer be independent of temperature. If the phase shift induced by the microwave interferometer was dependent on temperature, then the error signal produced by the interferometer would change with the temperature of the lab, thereby deteriorating the accuracy of our frequency lock.

To test this temperature stability we temporarily locked a voltage controlled oscillator (VCO)

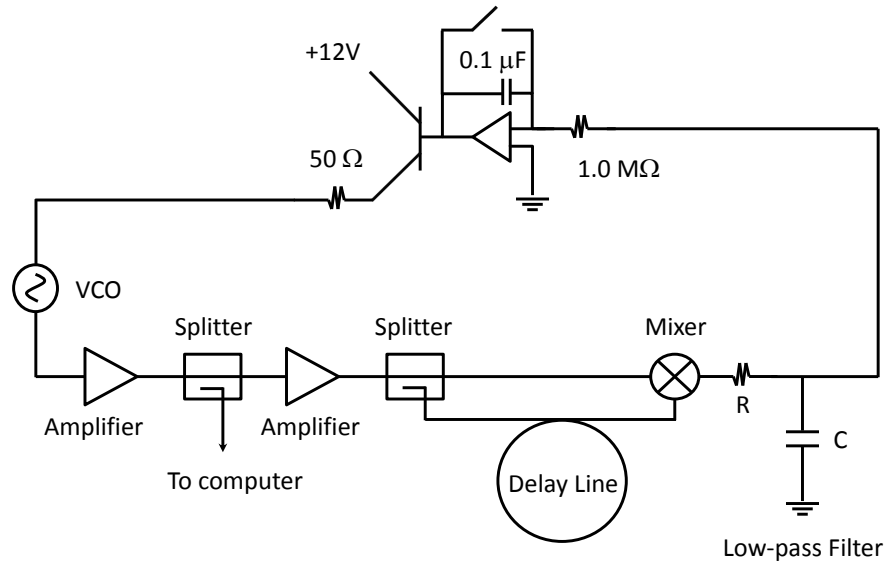


**Figure 2.2** Layout for interferometer during diagnostic tests. A single stage integrator is added to create a phase-locked loop

to a zero crossing of the interferometer's output . We used a simple negative feedback system to achieve this, as shown in Fig 2.2. For our particular cable lengths the VCO's output was locked at about 43.2 MHz when the feedback circuit was engaged. A thermistor was also installed thereby enabling us to monitor the temperature changes of the interferometer.

This system allowed us to test how the temperature influenced the interferometer's stability, because if the interferometer's phase changed, the feedback circuit would change the VCO's frequency to compensate. By measuring the change in the VCO's frequency we could determine how much the interferometer's phase changed.

Fig. 2.3 shows the frequency excursion as a function of thermistor resistance (and therefore temperature). We discovered that the co-axial cable has geometric dependence on temperature. As

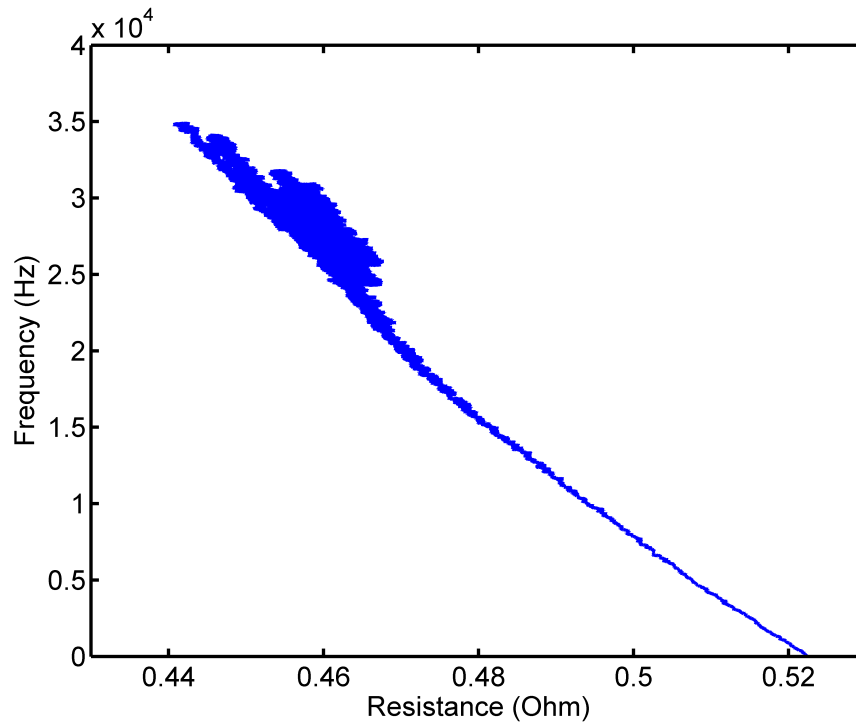


**Figure 2.3** The output frequency after the VCO plotted against the resistance of a thermistor installed in the Interferometer. The resistance is inversely proportional to temperature. The resistance values plotted represent typical temperature fluctuations in the lab due to the air conditioner. The output frequency after the VCO shows a linear dependence on the temperature (represented here as the resistance of the thermistor) of the apparatus. This can be explained by the geometric dependence of the co-axial cable on temperature. Temperature changes induce relative cable length changes, which in turn cause changes in the interference of the two signals, which likewise cause changes in the output frequency of the VCO.

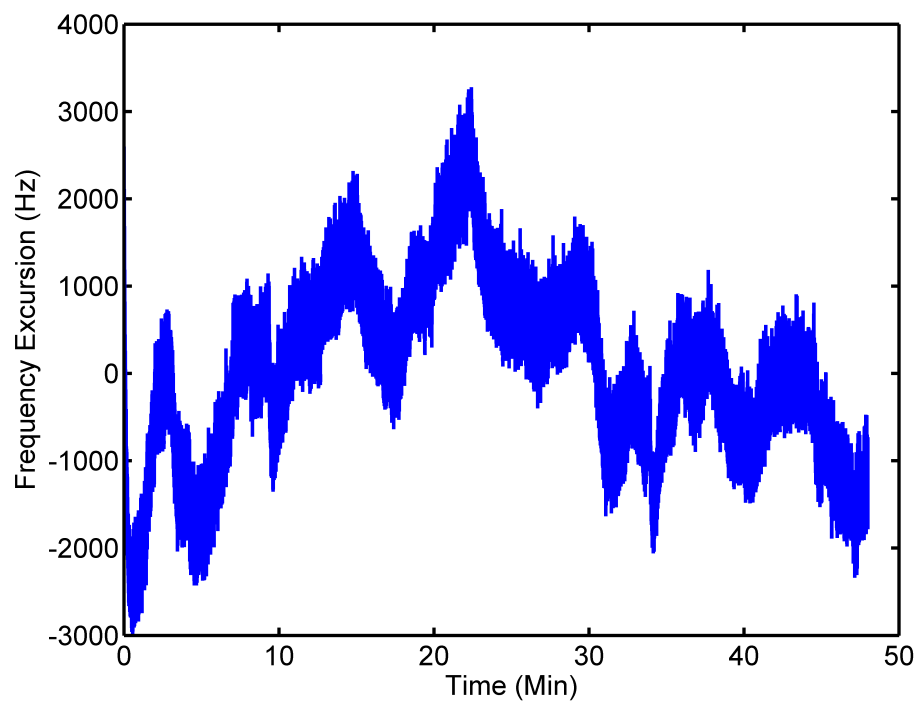


**Figure 2.4** The frequency excursion of the VCO before temperature controlling the interferometer. The std is  $1.0 \times 10^3$  Hz for a 50 min time interval (approx 5 K data points) after a linear fit to temperature.

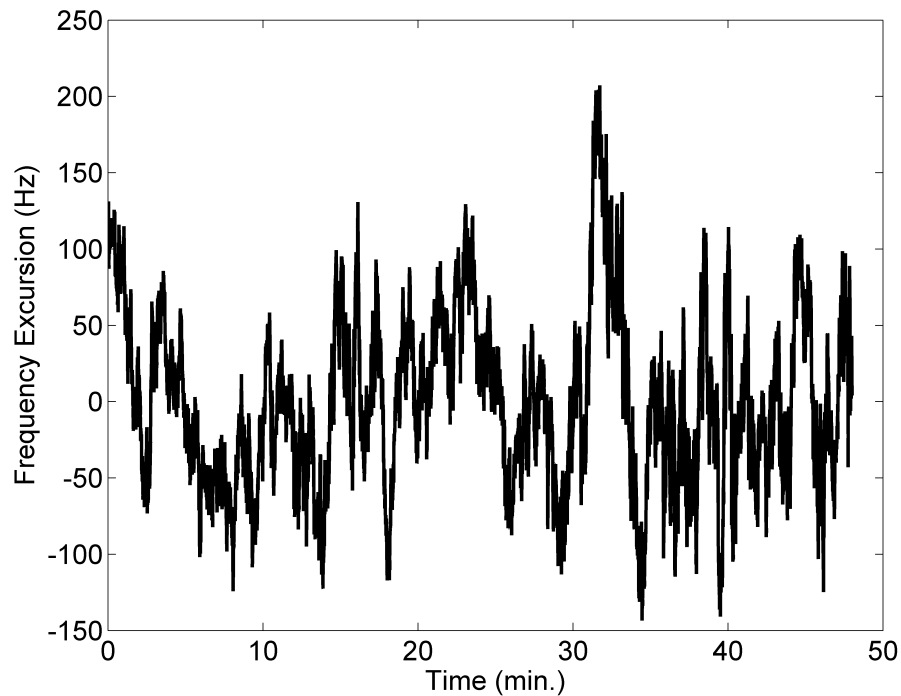


**Figure 2.5** The frequency excursion of the VCO after temperature controlling. The std is reduced to 56.8 for a 50 min time interval (approx 5 K data points) after a linear fit to temperature.

the temperature in the lab changes due to the air conditioner, the relative path lengths change as well as the phase of the output signal. This then writes frequency excursions onto the VCO. We see a standard deviation (std) of  $1.0 \times 10^3$  Hz for the VCO frequency excursion from 43.2 MHz for 50 minutes worth of data after a linear fit to temperature, as shown in Fig. 2.4.

To overcome the excursions caused by this dependence on temperature, we installed two Peltier devices on the bottom of the 1/4 in. aluminum plate to which the individual electronics (shown in Fig 2.2) were mounted. These devices kept the interferometer at a more stable temperature. We then placed this plate inside an aluminum box, which served as the heat sink for the Peltiers. We also mounted insulating foam around the entire exterior of the box. The results of our efforts can be seen in Fig. 2.5. The std is now reduced to 56.8 Hz for a similarly long test. Once the

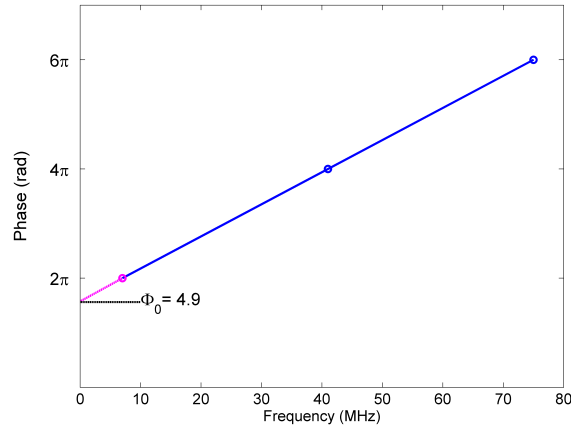


**Figure 2.6** Frequency of the beat note as a function of the interferometer's phase shift. Circles represent "0" crossings as we scanned from 5 to 80 MHz. The dotted line shows our extrapolation to determine  $\Phi_0$ .

interferometer's stability was characterized, we removed the VCO and negative feedback circuit.

Fundamental to the interferometer's proper function is its phase shift. If we let our error signal be represented as  $\cos(\Phi)$ , then the total induced phase shift is

$$\Phi = \Phi_0 + \frac{2\pi n(L_1 - L_2)}{\lambda},$$

where  $\Phi$  is the total interferometer phase shift,  $\Phi_0$  is the phase shift induced by both the splitter and mixer, and  $\frac{2\pi n(L_1 - L_2)}{\lambda}$  is the phase shift induced by the different lengths of cable. Although the phase shift induced by the different cable lengths is dependent on their relative length and the frequency of the beat note,  $\Phi_0$  is fixed and determined experimentally. We used a function generator to produce various beat note frequencies and recorded when the interferometer's output voltage went to zero. Since frequency and phase shift are linearly related, we plotted phase as a function of frequency and extrapolated  $\Phi_0$ . Fig. 2.6 shows the results. The y-intercept is the phase that is induced independent of the beat note frequency and relative cable lengths ( $\Phi_0$ ).

# Chapter 3

## Results

### 3.1 Frequency Noise Measurements

Since we want to know how the injection locking process affects the frequency noise of the amplified seed laser, we chose to first take the diode seed laser and make it co-linear with the commercial Ti:sapphire laser. The beat note produced by the interference of their electric fields is shown in Fig. 3.1. The red and blue side bands at 270 kHz are a result of the PDH feedback lock and are not inherent in either laser. The FWHM is 65 kHz.

Now that we know the frequency noise of our seed laser, we determined how it changed after amplification. Consequently, we injection-locked our diode seed laser to our home-built Ti:sapphire laser and overlapped its output with the commercial Ti:sapphire laser. The beat note produced by the interference of their electric fields is shown in Fig 3.2. The side bands are no longer visible because they have been encompassed by the frequency noise. The FWHM is 300 kHz. As a result of injection locking, the frequency noise has increased five fold relative to the commercial Ti:sapphire laser. This increased noise can likely be accounted for in part by the phase noise of the diode laser [3]. It should be noted, however, that a 300 kHz linewidth laser is still

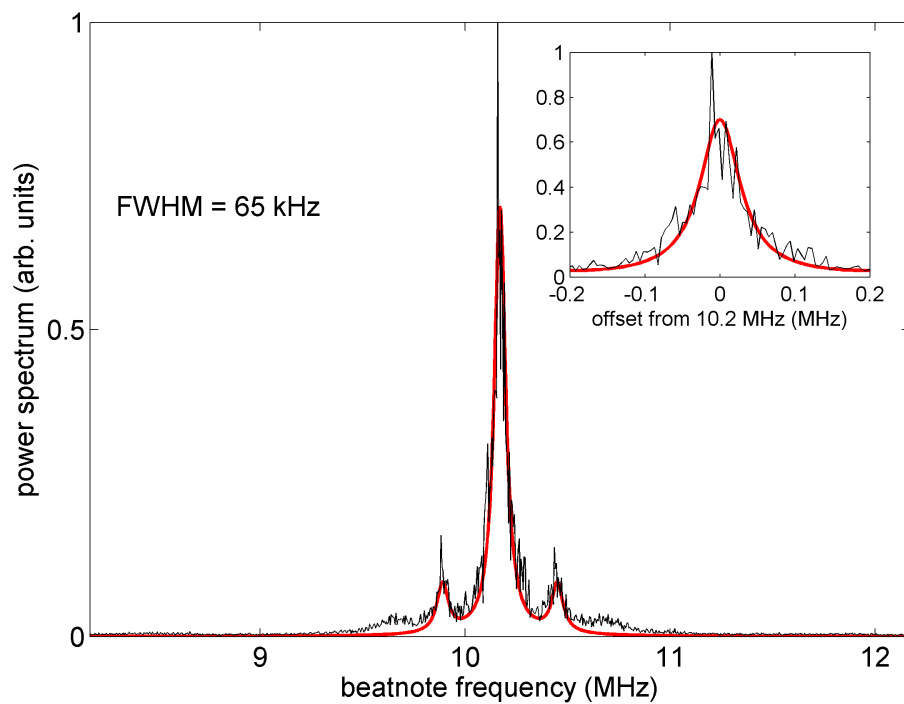


**Figure 3.1** The Frequency noise of the beat note between the diode seed and commercial Ti:sapphire lasers. The red line is a Lorentzian fit to the data. The FWHM is 65 kHz. Inset is the same data with a window range which excludes the side bands from the feedback lock.

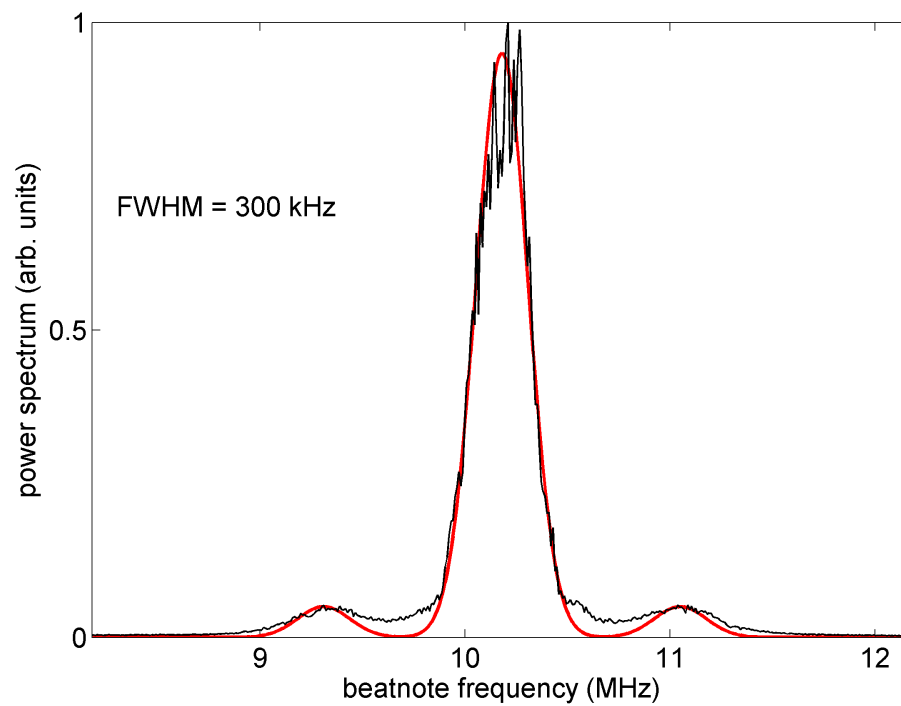


**Figure 3.2** The frequency noise of the beat note between the injection-locked Ti:sapphire and commercial Ti:sapphire. The red line is a Lorentzian fit to the data. The FWHM is 300 kHz.

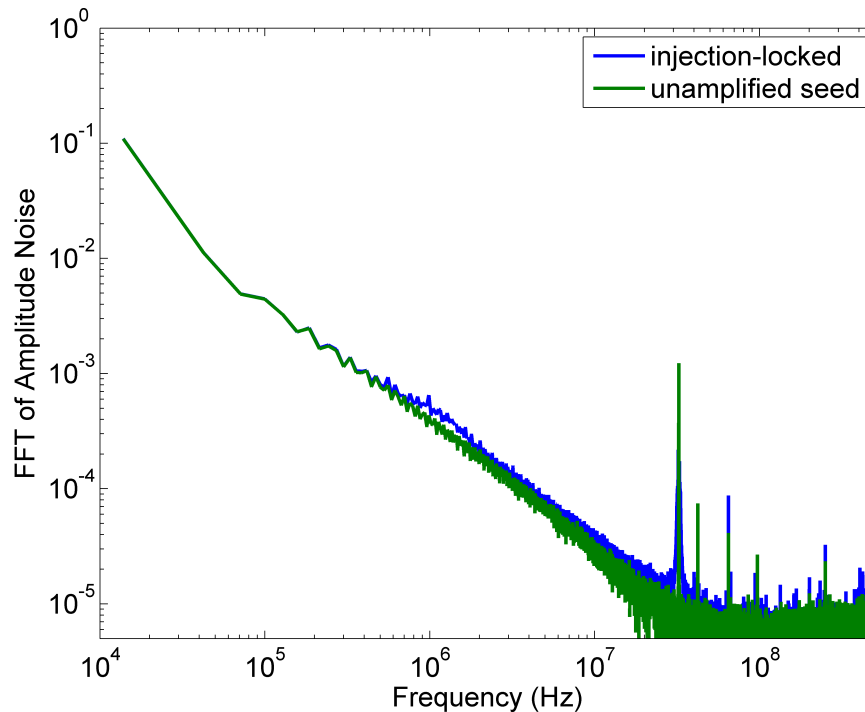


**Figure 3.3** The amplitude noise of the injection-locked laser compared with the amplitude noise of the unamplified seed laser, both normalized to the injection-locked amplitude mean, with 80 mW seed power. The rms noise is 1.0%. At 1 MHz the amplitude noise increases substantially compared to the seed laser.

considered a very stable laser in the optics community. This frequency noise would not preclude the use of this laser in most quantum optical experiments.

## 3.2 Amplitude Noise Measurements

Since we also want to know how the injection locking process affects the amplitude noise of the seed laser, we measure the amplitude noise of the seed laser alone. The Fourier transform of the data acquired by our photodetector in this measurement is shown in green (bottom curve) in Fig. 3.3. We then measure the amplitude noise of the amplified seed after injection-locking to our home-built Ti:sapphire cavity. The Fourier transform of the resulting data is shown in blue (top

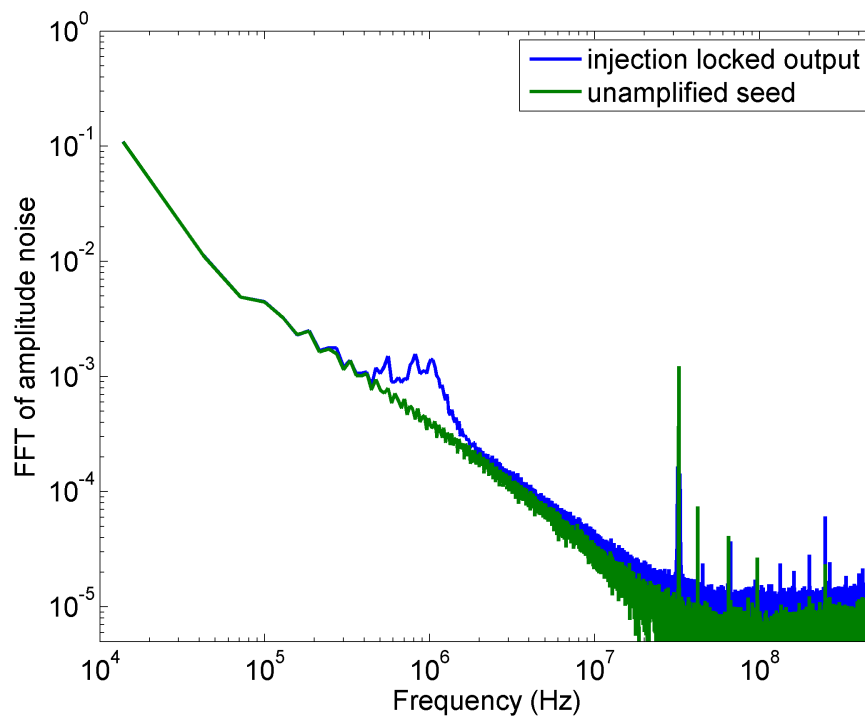


**Figure 3.4** The amplitude noise of the injection-locked laser compared with the amplitude noise of the unamplified seed laser, both normalized to the injection-locked amplitude mean, with 15 mW seed power. The rms noise has increased to 1.7%. The noise found in the 1 MHz regime increases when seed power decreases.

curve) in Fig. 3.3. The rms noise relative to the unamplified seed is 1.0 %. Again, this low noise level would not preclude the use of this laser in most quantum optics experiments.

It has been claimed that the amplitude noise induced by injection locking can not be controlled using conventional feedback methods [3]. Our initial amplitude noise data, mentioned above, is evidence to the contrary. With our PDH feedback system installed (perhaps the most popular conventional feedback method) we observed only 1.0 % rms noise as a result of amplification. In fact, the majority of the noise appears to take place between 1-10 MHz. To further demonstrate that our feedback system was working, we decided to operate our home-built laser in a regime where we knew it would perform more poorly (see section 3.3). If the amplitude noise increased when we entered this new regime then we would know that the feedback method was responsible.

To test this hypothesis we decreased the power of the seed laser being injected into our home-built Ti:sapphire cavity from 80 mW to 15 mW, which is the approximate seed power threshold of our Ti:sapphire cavity. The results are shown in Fig. 3.4. The amplitude noise is now 1.7 %. The noise has increased especially in the 1-10 MHz regime.

### 3.3 Discussion: Regenerative Amplifier Model

If we model our Ti:sapphire cavity as a regenerative amplifier, then the gain for the electric field of a weak beam reflecting from the high power laser cavity can be written as [1]

$$g(\omega_1) = \frac{\gamma_e}{i(\omega_0 - \omega_1)},$$

where  $\gamma_e$  is the cold cavity decay rate,  $\omega_0$  is the frequency of the field inside the laser cavity, and  $\omega_1$  is the seed laser frequency. Consequently,  $g(\omega_1)$  is dependent on the performance of the feedback lock, which minimizes the difference between  $\omega_0$  and  $\omega_1$ .

Furthermore, we can relate the performance of the feedback lock and the seed power by

$$\Delta\omega = 2\gamma_e \sqrt{\frac{I_1}{I_0}},$$

where  $I_1$  and  $I_0$  are the respective input (seed) and output intensities of the Ti:sapphire cavity. As the seed intensity decreases the precision of the feedback lock must increase or else there will be an increase in amplitude noise. The increased amplitude noise in the 1-10 MHz regime, which was observed as the seed power was decreased, is evidence of this relationship. This increase in amplitude noise suggests that at least some portion of the noise is a result of a feedback lock limitation. There appears to be a phase shift in the feedback system from 1-10 MHz which causes it to perform poorly in this regime.

### 3.4 Conclusion

Similar to [3], we find that injection locking a Ti:sapphire laser with a diode laser produces an increase in amplitude noise. We have also shown that this noise is dependent on the characteristics of the PDH feedback lock. Reference [3] based their phase-to-amplitude noise conversion theory on their observation of increased amplitude noise when the free running cavity is locked to the seed. Although we also observed this phenomena, we found that the amplitude noise is highly dependent on the PDH lock characteristics. Contrary to [3], we have shown that this amplitude noise can be suppressed using a conventional technique such as the PDH lock.

In addition, we have shown that the frequency noise also increases. It is interesting to compare our work with that of [6]. Here, a Ti:sapphire cavity is pumped with 19 W and produces 5.5 W output light. Although this is a higher power regime, and the authors underwent a heroic effort to stabilize the frequency of the diode seed output, they also observed the diode seed's frequency noise increase to the kHz level. Such observations suggest that there is some fundamental frequency noise inherent in injection locking. The source of this fundamental noise is still unclear.

It would be interesting to seed our Ti:sapphire cavity with a laser whose phase noise is known to be far less than our current seed diode laser. A measurement of the amplitude noise under

such conditions would be most revealing as to the influence of the seed laser's phase noise on the amplified lasers' amplitude noise.

This work shows that injection locking has limitations. However, those limitations do not preclude such systems from being powerful tools in quantum optic experiments [2].

# Bibliography

- [1] E. A. Cummings, M. S. Hicken, and S. D. Bergeson, “Demonstration of a 1-W injection-locked continuous-wave titanium:sapphire laser,” *Appl. Opt.* **41**, 7583–7587 (2002).
- [2] D. A. Thrasher, M. Burbidge, M. N. Conde, and S. D. Bergeson, “Comments on ‘Intensity Noise of an injection-locked Ti:sapphire laser: analysis of the phase-noise-to-amplitude-noise conversion’,” *J. Opt. Soc. Am. B* **28**, 1553–1555 (2011).
- [3] J. Belfi, I. Galli, G. Giusfredi, and F. Marin, “Intensity noise of an injection-locked Ti:sapphire laser: analysis of the phase-noise-to-amplitude-noise conversion,” *J. Opt. Soc. Am. B* **23**, 1276–1286 (2006).
- [4] R. W. P. Drever, J. L. Hall, F. V. Kowalski, J. Hough, G. M. Ford, A. J. Munley, and H. Ward, “Laser phase and frequency stabilization using an optical resonator,” *Appl. Phys. B* **31**, 97–105 (1983).
- [5] U. Schunemann, H. Engler, R. Grimm, M. Weidemuller, and M. Zielonkowski, “Simple scheme for tunable frequency offset locking of two lasers,” *Rev. Sci. Instrum.* **70** (1999).
- [6] S. Chiow, S. Herrmann, H. Müller, and S. Chu, “6W, 1 kHz linewidth, tunable continuous-wave near-infrared laser,” *Opt. Express* **17**, 5246–5250 (2009).

# Index

- bandwidth
  - amplifier, 2
  - detector, 6
- cavity
  - power amplifier, 2
- error signal, 13
- feedback
  - negative, 5, 9
- linear dependence
  - phase and frequency, 13
  - Temperature, 10
- Peltier, 12
- Pound-Drever-Hall (PDH), 2, 14, 19, 20
- resonance, 2
- seed
  - amplitude noise, 17
  - frequency noise, 14
  - threshold, 19
- stability
  - beat note, 4
  - interferometer, 9
- zero crossing, 9